Chapter 6: Viscous Flow in Ducts

6.1 Laminar Flow Solutions

Entrance, developing, and fully developed flow

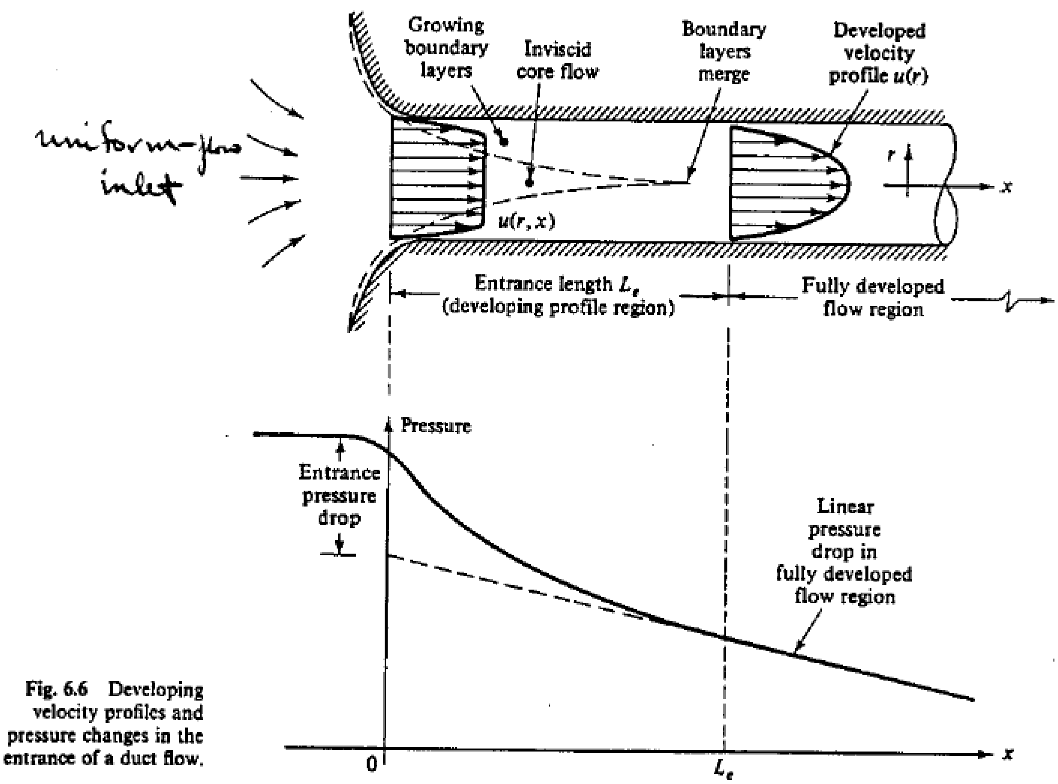

Fig. 6.6 Developing velocity profiles and pressure changes in the entrance of a duct flow.

$$Le = f\,(D, V, \rho, \mu)$$

$$\Pi_i \ theorem \rightarrow L_e/D = f\,(\mathrm{Re}) \text{ f(Re) from AFD and EFD}$$

Laminar Flow: $\mathrm{Re}_{crit} \sim 2000$ $\mathrm{Re} < \mathrm{Re}_{crit}$ laminar

$L_e / D \cong .06\,\mathrm{Re}$ $\mathrm{Re} > \mathrm{Re}_{crit}$ unstable

$\mathrm{Re} > \mathrm{Re}_{trans}$ turbulent

$L_{e\max} = .06\,\mathrm{Re}_{crit}\, D \sim 138D$

Max L_e for laminar flow

Turbulent flow:

Re	L_e/D
4000	18
10^4	20
10^5	30
10^6	44
10^7	65
10^8	95

$$L_e / D \sim 4.4 \mathrm{Re}^{1/6}$$

(Relatively shorter than for laminar flow)

Laminar vs. Turbulent Flow

Hagen 1839

Hagen 1839 noted difference in $\Delta p = \Delta p(u)$ but could not explain two regimes

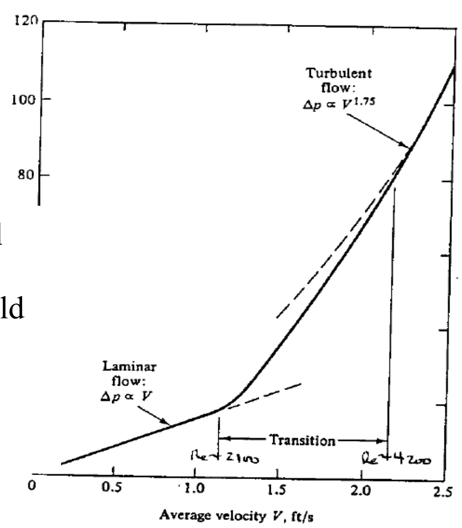

evidence of transition for water flow in a ½-in smooth pipe 10 ft long.

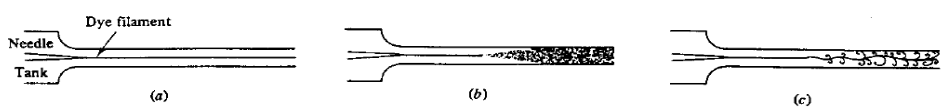

laminar turbulent spark photo

Reynolds 1883 showed difference depends on $Re = \frac{VD}{\nu}$

Laminar Turbulent Spark photo

Reynolds 1883 showed that the difference depends on Re = VD/ν

Laminar pipe flow:

1. CV Analysis

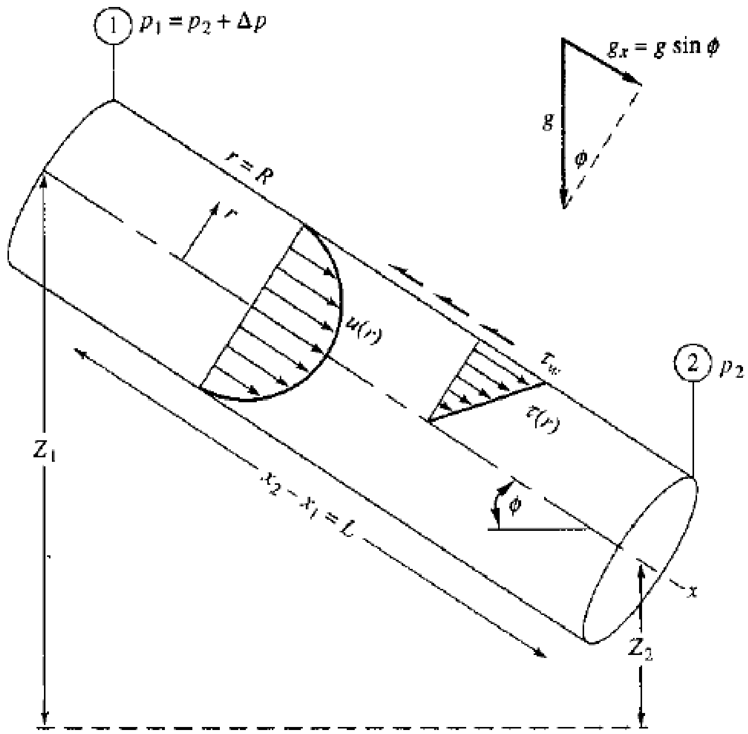

Fig. 6.7 Control volume of steady, fully developed flow between two sections in an inclined pipe.

Continuity:

$$0 = \int_{CS} \rho \underline{V} \cdot \underline{dA} \rightarrow \rho Q_1 = \rho Q_2 = const.$$

$$i.e. V_1 = V_2 \quad \text{since} \quad A_1 = A_2,\ \rho = const., \text{and } V = V_{ave}$$

Momentum:

$$\sum F_x = \underbrace{(p_1 - p_2)}_{\Delta p}\pi R^2 - \tau_w 2\pi RL + \underbrace{\gamma\pi R^2 L}_{W}\underbrace{\sin\phi}_{\Delta z/L} = \underbrace{\dot{m}(\beta_2 V_2 - \beta_1 V_1)}_{=0}$$

$$\Delta p \pi R^2 - \tau_w 2\pi RL + \gamma\pi R^2 \Delta z = 0$$

$$\Delta p + \gamma\Delta z = \frac{2\tau_w L}{R}$$

$\Delta h = h_1 - h_2 = \Delta(p/\gamma + z) = \frac{2\tau_w}{\gamma}\frac{L}{R}$

or

$$\tau_w = \frac{R\gamma}{2}\frac{\Delta h}{L} = -\frac{R\gamma}{2}\frac{dh}{dx}$$
$$= -\frac{R}{2}\frac{d}{dx}(p + \gamma z)$$

For fluid particle control volume:

$$\tau = -\frac{r}{2}\frac{d}{dx}(p + \gamma z)$$

i.e. shear stress varies linearly in r across pipe for either laminar or turbulent flow

Energy:

$$\frac{p_1}{\gamma} + \frac{\alpha_1}{2g}V_1 + z_1 = \frac{p_2}{\gamma} + \frac{\alpha_2}{2g}V_2 + z_2 + h_L$$

$$\Delta h = h_L = \frac{2\tau_w}{\gamma}\frac{L}{R}$$

$\therefore$ once τ_w is known, we can determine pressure drop

In general,

$$\tau_w = \tau_w(\rho, V, \mu, D, \varepsilon)$$

roughness

Π_i Theorem

$$\frac{8\tau_w}{\rho V^2} = f = friction\ \ factor = f(\mathrm{Re}_D, \varepsilon / D)$$

where $\mathrm{Re}_D = \frac{VD}{\upsilon}$

$$\Delta h = h_L = f\frac{L}{D}\frac{V^2}{2g}$$ Darcy-Weisbach Equation

f (Re_D, ε/D) still needs to be determined. For laminar flow, there is an exact solution for *f* since laminar pipe flow has an exact solution. For turbulent flow, approximate solution for *f* using log-law as per Moody diagram and discussed later.

2. Differential Analysis

Continuity:

$$\nabla \cdot \underline{V} = 0$$

Use cylindrical coordinates (r, θ, z) where z replaces x in previous CV analysis

$$\frac{1}{r}\frac{\partial}{\partial r}(rv_r) + \frac{1}{r}\frac{\partial}{\partial \theta}(v_\theta) + \frac{\partial v_z}{\partial z} = 0$$

$$\text{where } \underline{V} = v_r\widehat{e_r} + v_\theta\widehat{e_\theta} + v_z\widehat{e_z}$$

Assume $v_\theta = 0$ i.e. no swirl and fully developed flow $\frac{\partial v_z}{\partial z} = 0$, which shows v_r = constant = 0 since $v_r(R) = 0$

$$\therefore \underline{V} = v_z\widehat{e_z} = u(r)\widehat{e_z}$$

Momentum:

$$\rho\frac{D\underline{V}}{Dt} = \rho\frac{\partial\underline{V}}{\partial t} + \rho\underline{V}\cdot\nabla\underline{V} = -\nabla(\mathrm{p} + \gamma\mathrm{z}) + \mu\nabla^2\underline{V}$$

Where

$$\underline{V}\cdot\nabla = v_r\frac{\partial}{\partial r} + v_\theta\frac{1}{r}\frac{\partial}{\partial\theta} + v_z\frac{\partial}{\partial z}$$

z equation:

$$\rho\left[\frac{\partial u}{\partial t} + \underline{V}\cdot\nabla u\right] = -\frac{\partial}{\partial z}(p+\gamma z) + \mu\nabla^2 u$$

$$0 = \underbrace{-\frac{\partial}{\partial z}(p+\gamma z)}_{f(z)} + \underbrace{\mu\frac{1}{r}\frac{\partial}{\partial r}\left(r\frac{\partial u}{\partial r}\right)}_{f(r)}$$

$\therefore$ both terms must be constant

$$\frac{\mu}{r}\frac{\partial}{\partial r}(r\frac{\partial u}{\partial r})=\frac{\partial \hat{p}}{\partial z}$$

$$\Rightarrow r\frac{\partial u}{\partial r}=\frac{1}{2\mu}\frac{\partial \hat{p}}{\partial z}r^2+A$$

$$\Rightarrow \frac{\partial u}{\partial r}=\frac{1}{2\mu}\frac{\partial \hat{p}}{\partial z}r+A$$

$$\Rightarrow u=\frac{1}{4\mu}\frac{\partial \hat{p}}{\partial z}r^2+A\ln r+B \qquad \hat{p}=p+\gamma$$

$u(r=0)$ *finite* → $A = 0$

$u\ (r=R) = 0$ → $B=-\frac{R^2}{4\mu}\frac{d\hat{p}}{dz}$

$$u(r)=\frac{r^2-R^2}{4\mu}\frac{d\hat{p}}{dz} \qquad u_{\max}=u(0)=-\frac{R^2}{4\mu}\frac{d\hat{p}}{dz}$$

$$\tau=\mu\left[\frac{\partial v_r}{\partial z}+\frac{\partial u}{\partial r}\right]=\mu\frac{\partial u}{\partial r} \quad \textit{fluid shear stress}$$

$$=\frac{r}{2}\frac{\partial \hat{p}}{\partial z}$$

$$\tau_w=\mu\left.\frac{\partial u}{\partial y}\right|_{y=0}=-\mu\left.\frac{\partial u}{\partial r}\right|_{r=R}=-\frac{R}{2}\frac{\partial \hat{p}}{\partial z} \quad \text{As per CV analysis}$$

$$y=R-r,\ \frac{du}{dy}=\frac{dr}{dy}\frac{du}{dr}=-\frac{du}{dr}$$

$$Q = \int_0^R u(r) 2\pi r\, dr = \frac{-\pi R^4}{8\mu}\frac{d\hat{p}}{dz} = \frac{1}{2}u_{\max}\pi R^2$$

$$V_{ave} = \frac{Q}{\pi R^2} = \frac{1}{2}u_{\max} = \frac{-R^2}{8\mu}\frac{d\hat{p}}{dz}$$

Substituting $V = V_{ave}$

$$f = \frac{8\tau_w}{\rho V^2}$$

$$\tau_w = -\frac{R}{2} \times \frac{8\mu V_{ave}}{-R^2} = \frac{4\mu V_{ave}}{R} = \frac{8\mu V}{D}$$

$$\boxed{f = \frac{64\mu}{\rho D V} = \frac{64}{\mathrm{Re}_D}}$$

or

$$\boxed{C_f = \frac{\tau_w}{\frac{1}{2}\rho V^2} = \frac{f}{4} = \frac{16}{\mathrm{Re}_D}}$$

$$\Delta h = h_L = f\frac{L}{D}\frac{V^2}{2g} = \frac{64\mu}{\rho D V} \times \frac{L}{D} \times \frac{V^2}{2g} = \frac{32\mu L V}{\rho g D^2} \quad \propto V$$

$$\textit{for } \Delta z = 0 \quad \rightarrow \quad \Delta p \propto V$$

Both f and C_f based on V^2 normalization, which is appropriate for turbulent but not laminar flow. The more appropriate case for laminar flow is:

$$\boxed{Poiseuille\#\ (P_0)\begin{cases} P_{0_{c_f}} = C_f \operatorname{Re} = 16 \\ P_{0_f} = f \operatorname{Re} = 64 \end{cases}} \qquad \textit{for pipe flow}$$

Compare with previous solution for flow between parallel plates with $\hat{p}$

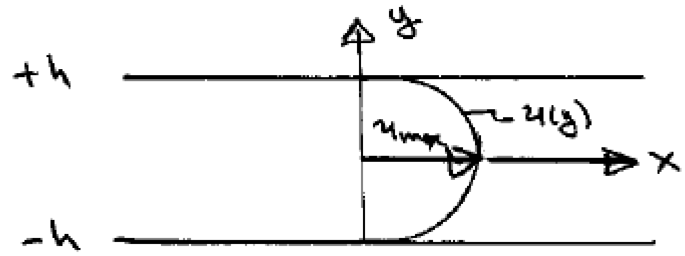

$$u = u_{\max}\left(1 - \left(\frac{y}{h}\right)^2\right) \qquad u_{\max} = \frac{-h^2}{2\mu}\hat{p}_x$$

$$q = \frac{4}{3}hu_{\max} = \frac{2h^3}{3\mu}\left(-\hat{p}_x\right)$$

$$V_{avg} = \frac{q}{2h} = \frac{h^2}{3\mu}(-\widehat{p_x}) = \frac{2}{3}u_{max}$$

$$\tau_w = {}^{3\mu V}\!\big/_{h}$$

$$\boxed{f=\frac{24\mu}{\rho Vh}=\frac{48}{\mathrm{Re}_{2h}}=\frac{96}{\underbrace{\mathrm{Re}_{4h}}_{\mathrm{Re}_{D_h}}}}$$

$$\boxed{\begin{array}{l} C_f=f/4\Rightarrow \\ C_f=\dfrac{6\mu}{\rho Vh}=\dfrac{12}{\mathrm{Re}_{2h}}=\dfrac{24}{\underbrace{\mathrm{Re}_{4h}}_{\mathrm{Re}_{D_h}}} \end{array}}$$

$$\boxed{Poiseuille\#\,(P_0)\begin{cases} P_{0c_f}=C_f\,\mathrm{Re}_{D_h}=24 \\ P_{0f}=f\,\mathrm{Re}_{D_h}=96 \end{cases}}$$

Same as pipe other than constants!

$$\boxed{\frac{P_{0c_f\ pipe}}{P_{0c_f\ channel\ based\ on\ D_h}}=\frac{P_{0\,f\ pipe}}{P_{0\,f\ channel\ based\ on\ D_h}}=\frac{16}{24}=\frac{64}{96}=\frac{2}{3}}$$

Exact laminar solutions are available for any "arbitrary" cross section for laminar steady fully developed duct flow

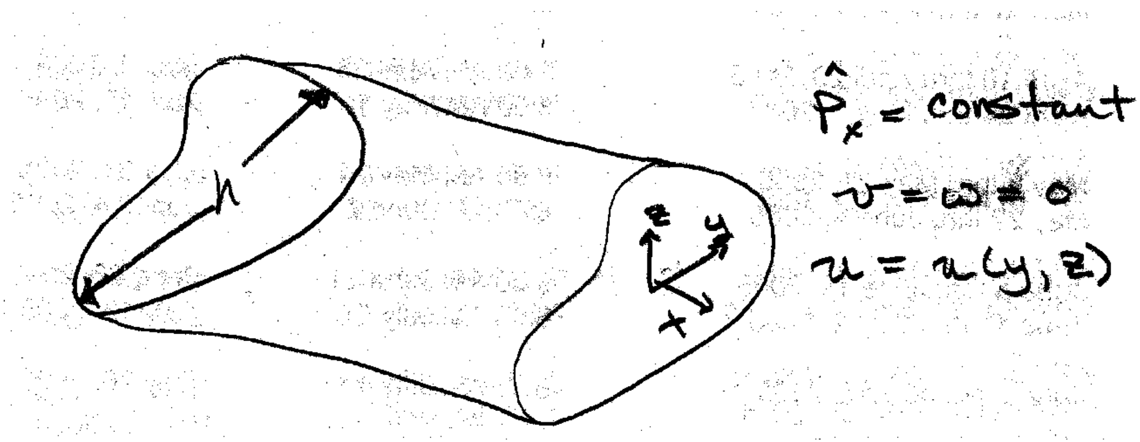

BVP

$$u_x = 0$$

$$0 = -\hat{p}_x + \mu(u_{YY} + u_{ZZ})$$

$$u(h) = 0$$

Re only enters through stability and transition

$$y^* = y/h \qquad z^* = z/h \qquad u^* = u/U \qquad U = \frac{h^2}{\mu}(-\hat{p}_x)$$

Related u_{max}

$\nabla^2 u = -1$ *Poisson equation*

u(1) = 0 *Dirichlet boundary condition*

Can be solved by many methods such as complex variables and conformed mapping, transformation into Laplace equation by redefinition of dependent variables, and numerical methods.

Table 6.4 Laminar Friction Constants $f\mathrm{Re}$ for Rectangular and Triangular Ducts

Rectangular		Isosceles triangle	

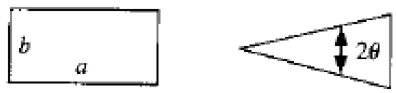

b/a	$f\mathrm{Re}_{D_h}$	θ, deg	$f\mathrm{Re}_{D_h}$
0.0	96.00	0	48.0
0.05	89.91	10	51.6
0.1	84.68	20	52.9
0.125	82.34	30	53.3
0.167	78.81	40	52.9
0.25	72.93	50	52.0
0.4	65.47	60	51.1
0.5	62.19	70	49.5
0.75	57.89	80	48.3
1.0	56.91	90	48.0

Table 6.3 Laminar Friction Factors for a Concentric Annulus

b/a	$f\,\mathrm{Re}_{D_h}$	$D_{\mathrm{eff}}/D_h = 1/\zeta$
0.0	64.0	1.000
0.00001	70.09	0.913
0.0001	71.78	0.892
0.001	74.68	0.857
0.01	80.11	0.799
0.05	86.27	0.742
0.1	89.37	0.716
0.2	92.35	0.693
0.4	94.71	0.676
0.6	95.59	0.670
0.8	95.92	0.667
1.0	96.0	0.667

3-3.3 Noncircular Ducts

Since Eq. (3-32) for fully developed duct flow is equivalent to a classic Dirichlet problem, it is not surprising that an enormous number of exact solutions are known for noncircular shapes, as reviewed by Berker (1963). Some of these shapes are shown in Fig. 3-9. Each solution is fascinating, but our mathematical ardor should be dampened somewhat by the practical fact that limaçon-shaped ducts, for example, are not commercially available at present. Nevertheless we list a few of these solutions because they lead to a valuable approximate principle, the *hydraulic radius*. The velocity distribution would suffice, but the volume rate of flow is a bonus.

Elliptical section: $y^2/a^2 + z^2/b^2 \le 1$:

$$u(y,z) = \frac{1}{2\mu}\left(-\frac{d\hat{p}}{dx}\right)\frac{a^2b^2}{a^2+b^2}\left(1-\frac{y^2}{a^2}-\frac{z^2}{b^2}\right)$$

$$Q = \frac{\pi}{4\mu}\left(-\frac{d\hat{p}}{dx}\right)\frac{a^3b^3}{a^2+b^2} \tag{3-47}$$

Rectangular section: $-a \le y \le a,\ -b \le z \le b$:

$$u(y,z) = \frac{16a^2}{\mu\pi^3}\left(-\frac{d\hat{p}}{dx}\right)\sum_{i=1,3,5,\ldots}^{\infty}(-1)^{(i-1)/2}\left[1-\frac{\cosh(i\pi z/2a)}{\cosh(i\pi b/2a)}\right] \times \frac{\cos(i\pi y/2a)}{i^3} \tag{3-48}$$

$$Q = \frac{4ba^3}{3\mu}\left(-\frac{d\hat{p}}{dx}\right)\left[1-\frac{192a}{\pi^5 b}\sum_{i=1,3,5,\ldots}^{\infty}\frac{\tanh(i\pi b/2a)}{i^5}\right]$$

Equilateral triangle of side a: coordinates in Fig. 3-9:

$$u(y,z) = \frac{-d\hat{p}/dx}{2\sqrt{3}\,a\mu}\left(z-\frac{1}{2}a\sqrt{3}\right)(3y^2-z^2)$$

$$Q = \frac{a^4\sqrt{3}}{320\mu}\left(-\frac{d\hat{p}}{dx}\right) \tag{3-49}$$

Circular sector: $-\frac{1}{2}\alpha \le \theta \le +\frac{1}{2}\alpha,\ 0 \le r \le a$:

$$u(r,\theta) = \frac{d\hat{p}/dx}{4\mu}\left[r^2\left(1-\frac{\cos 2\theta}{\cos\alpha}\right)-\frac{16a^2\alpha^2}{\pi^3} \times \sum_{i=1,3,5,\ldots}^{\infty}(-1)^{(i+1)/2}\left(\frac{r}{a}\right)^i\frac{\cos(i\pi\theta/\alpha)}{i(i+2\alpha/\pi)(i-2\alpha/\pi)}\right]$$

$$Q = \frac{a^4}{4\mu}\left(-\frac{d\hat{p}}{dx}\right) \times \left[\frac{\tan\alpha-\alpha}{4}-\frac{32\alpha^4}{\pi^5}\sum_{i=1,3,5,\ldots}^{\infty}\frac{1}{i^2(i+2\alpha/\pi)^2(i-2\alpha/\pi)}\right] \tag{3-50}$$

Concentric circular annulus: $b \le r \le a$:

$$u(r) = \frac{-d\hat{p}/dx}{4\mu}\left[a^2-r^2+(a^2-b^2)\frac{\ln(a/r)}{\ln(b/a)}\right]$$

$$Q = \frac{\pi}{8\mu}\left(-\frac{d\hat{p}}{dx}\right)\left[a^4-b^4-\frac{(a^2-b^2)^2}{\ln(a/b)}\right] \tag{3-51}$$

This is but a sample of the wealth of solutions available. The formula for a concentric annulus is important in viscometry, with a measured Q being used to calculate μ. To increase the pressure drop, the clearance $(a-b)$ is held small, in which case Eq. (3-51) for Q becomes the difference between two nearly equal

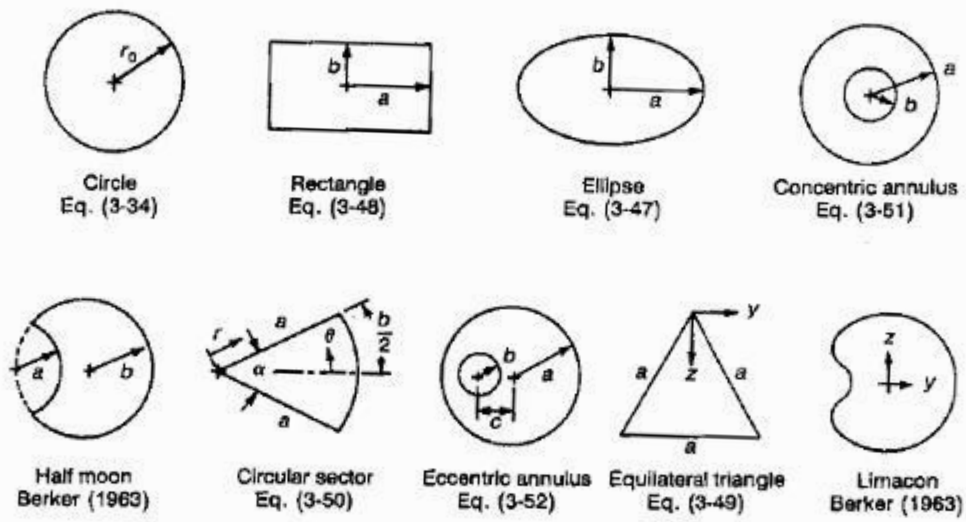

FIGURE 3-9
Some cross sections for which fully developed flow solutions are known; for still more, consult Berker (1963, pp. 67ff.) or Shah and London (1978).

numbers. However, if we expand the bracketed term [ ] in a series, the result is

$$(a^4 - b^4) - \frac{(a^2 - b^2)^2}{\ln(a/b)} = \frac{4}{3}b(a-b)^3 + \frac{2}{3}(a-b)^4 + \cdots + \mathcal{O}(a-b)^5$$

so that Q for small clearance is seen to be cubic in $(a - b)$.

The eccentric annulus in Fig. 3-9 has practical applications, as for example when a needle valve becomes misaligned. The solution was given by Piercy et al. (1933), using an elegant complex-variable method which transformed the geometry to a concentric annulus, for which the solution was already known, Eq. (3-51). We reproduce here only their expression for volume rate of flow:

$$Q = \frac{\pi}{8\mu}\left(-\frac{d\hat{p}}{dx}\right)\left[a^4 - b^4 - \frac{4c^2M^2}{\beta - \alpha} - 8c^2M^2\sum_{n=1}^{\infty}\frac{ne^{-n(\beta+\alpha)}}{\sinh(n\beta - n\alpha)}\right] \quad (3\text{-}52)$$

where $$M = (F^2 - a^2)^{1/2} \qquad F = \frac{a^2 - b^2 + c^2}{2c}$$

$$\alpha = \frac{1}{2}\ln\frac{F+M}{F-M} \qquad \beta = \frac{1}{2}\ln\frac{F-c+M}{F-c-M}$$

Flow rates computed from this formula are compared in Fig. 3-10 to the concentric result Q_{c-0} from Eq. (3-51). It is seen that eccentricity substantially increases the flow rate, the maximum ratio of Q/Q_{c-0} being 2.5 for a narrow annulus of maximum eccentricity. The curve for $b/a = 1$ can be derived from

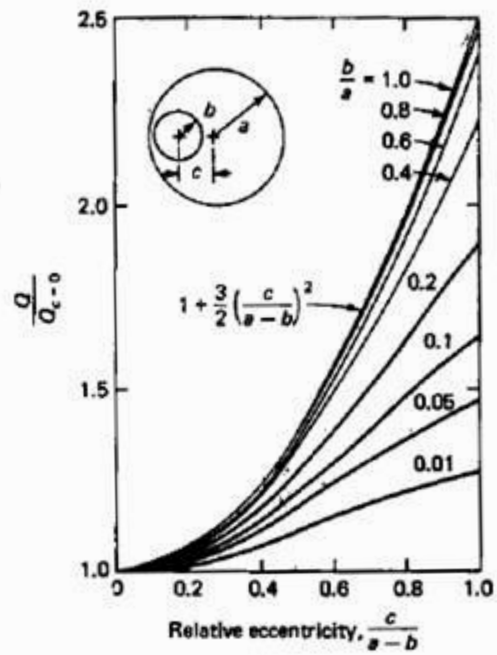

FIGURE 3-10
Volume flow through an eccentric annulus as a function of eccentricity, Eq. (3-52).

lubrication theory:

Narrow annulus:
$$\frac{Q}{Q_{c=0}} = 1 + \frac{3}{2}\left(\frac{c}{a-b}\right)^2 \tag{3-53}$$

The reason for the increase in Q is that the fluid tends to bulge through the wider side. This is illustrated for one case in Fig. 3-11, where the wide side develops a set of closed high-velocity streamlines. This effect is well known to piping engineers, who have long noted the drastic leakage that occurs when a nearly closed valve binds to one side.

3-3.4 The Concept of Hydraulic Diameter

The definition of λ proposed in Eq. (3-39) fails for a noncircular duct since τ_w varies around the perimeter. For example, in the equilateral-triangle duct, Eq.

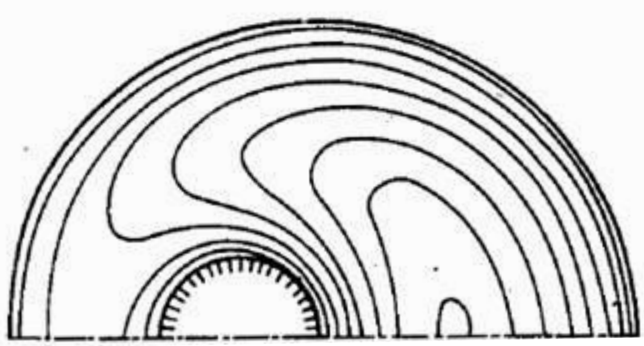

FIGURE 3-11
Constant-velocity lines for an eccentric annulus, $b/a = c/a = \frac{1}{4}$. [*After Piercy et al.* (1933).]